European Journal of Physics

PAPER

The hobbyhorse of magnetic systems: the Ising model

To cite this article: Eduardo Ibarra-García-Padilla *et al* 2016 *Eur. J. Phys.* **37** 065103

IOP Publishing European Journal of Physics
Eur. J. Phys. **37** (2016) 065103 (27pp) doi:10.1088/0143-0807/37/6/065103

The hobbyhorse of magnetic systems: the Ising model

Eduardo Ibarra-García-Padilla[1], **Carlos Gerardo Malanche-Flores**[2] and **Freddy Jackson Poveda-Cuevas**[1]

[1] Instituto de Física, Universidad Nacional Autónoma de México, Apartado Postal 20-364, México D.F. 01000, Mexico
[2] École Polytechnique Fédérale de Lausanne, Lausanne, VD, Switzerland

E-mail: eibarragp@fisica.unam.mx

Received 11 July 2016, revised 9 August 2016
Accepted for publication 22 August 2016
Published 26 September 2016

Abstract

In undergraduate statistical mechanics courses the Ising model always plays an important role because it is the simplest non-trivial model used to describe magnetic systems. The one-dimensional model is easily solved analytically, while the two-dimensional one can be solved exactly by the Onsager solution. For this reason, numerical simulations are usually used to solve the two-dimensional model. Keeping in mind that the two-dimensional model is the platform for studying phase transitions, it is usually an exercise in computational undergraduate courses because its numerical solution is relatively simple to implement and its critical exponents are perfectly known. The purpose of this article is to present a detailed numerical study of the second-order phase transition in the two-dimensional Ising model at an undergraduate level, allowing readers not only to compare the mean-field solution, the exact solution and the numerical one through a complete study of the order parameter, the correlation function and finite-size scaling, but to present the techniques, along with hints and tips, for solving it themselves. We present the elementary theory of phase transitions and explain how to implement Markov chain Monte Carlo simulations and perform them for different lattice sizes with periodic boundary conditions. Energy, magnetization, specific heat, magnetic susceptibility and the correlation function are calculated and the critical exponents determined by finite-size scaling techniques. The importance of the correlation length as the relevant parameter in phase transitions is emphasized.

Keywords: Ising model, phase transitions, Monte Carlo simulations, finite-size scaling

(Some figures may appear in colour only in the online journal)

1. Introduction

When the Ising model was first introduced it appeared that the greatly over-simplified representation of intermolecular forces on which the model is based would make it inapplicable to any real system. However, it seems that the essential features of cooperative phenomena do not depend on the details of intermolecular forces but on the mechanisms of propagation of long-range order, and the Ising model is a good first approximation to the problem [1].

Nowadays it is the most-well studied model in statistical mechanics, and although the Ising model is the simplest model used to describe a magnetic system it is also very versatile. For example, it can also be used to model the fluid critical point and binary alloy phase separation [2, 3], and variations of the Ising model have been used in high-energy physics to explore the behavior of simple lattice gauge theories [2, 4].

Despite the simplicity of the model, it was solved analytically in the one-dimensional (1D) case in 1925 by Ising [5] and in 1944 for a two-dimensional (2D) square lattice by Onsager [6]. It is worth mentioning that the 1D case does not exhibit a phase transition while the 2D case does. Also, although the 2D Ising model can be solved analytically, the three-dimensional (3D) version does not have an analytical solution [7] or at least no solution has yet been found. However, solutions of the model can be found by numerical methods in n-dimensional square lattices without huge complications, and for this reason it is usually presented as an exercise in textbooks [3, 8, 9] and in some undergraduate computational courses.

Even though the computational algorithms for solving the Ising model are 'simple' to program and are discussed and presented in textbooks [3, 8–10], recovering thermodynamic properties and critical phenomena is not as straightforward as it might seem. It is our aim to give the reader a complete approach to the problem of critical phenomena in the 2D Ising model. In order to do so, elementary phase transition theory, computational algorithms and finite-size scaling techniques are presented.

This article is organized as follows. In section 2 we introduce the Hamiltonian that is used to describe magnetic systems. Section 3 introduces phase transitions, the order parameter, the correlation function and the scaling hypothesis. Results from the mean-field and the exact solution are presented in section 4, while in section 5 the tools for the numerical solution are discussed. In section 6 the numerical results are presented with their benchmarks and those results are discussed in section 7, where the importance of the correlation length in phase transitions is emphasized. An example of the relevance of the correlation length is given in section 8 where the XY model is discussed. Suggested problems are given in section 9.

2. Magnetic systems

In describing the thermodynamics of magnetic systems a mean-field model called the Weiss molecular field theory is used. The Hamiltonian of the system is the Heisenberg Hamiltonian given by [11, 12]

$$\mathcal{H} = -\frac{J}{2}\sum_{\langle ij\rangle} \mathbf{s}_i \cdot \mathbf{s}_j - \mathbf{H} \cdot \sum_i \mathbf{s}_i, \tag{1}$$

where $\mathbf{H}$ is the applied external magnetic field and J is the coupling constant which measures the strength of the interaction between spins or magnetic moments $\mathbf{s}_i$. Ferromagnetic systems correspond to $J > 0$ and anti-ferromagnetic ones correspond to $J < 0$. Each spin has a fixed location on a lattice and is labelled by the index i, whereas the index $\langle ij\rangle$ indicates that only nearest-neighbour interactions are considered.

The net magnetization of the system is given by,

$$\mathbf{M} = \sum_i \mathbf{s}_i. \tag{2}$$

It is important to stress that setting J as a constant in the Hamiltonian is a simplification. The interaction between the spins J_{ij} is called the exchange interaction and is an extremely complicated quantum phenomenon (see for example Mattis's book [13]).

The temperature T will be introduced in the model through the partition function Z given by,

$$Z = \mathrm{Tr}\,(\mathrm{e}^{-\mathcal{H}/k_\mathrm{B}T}), \tag{3}$$

where k_B is the Boltzmann constant. The partition function is linked with the free energy F by the following relation,

$$F = -k_\mathrm{B}T \ln Z. \tag{4}$$

As free energy is a thermodynamic potential, all thermodynamic properties can be inferred from it such as specific heat and magnetic susceptibility. The introduction of temperature in the model will become clearer in section 5 where the numerical solution is discussed.

In the Ising model, the spin values are restricted to $\mathbf{s}_i = \pm 1\ \mathbf{e}_z$, where $\mathbf{e}_z$ is the unitary vector of the z-component, thus the vector problem is reduced to a classical scalar Hamiltonian. The 1D Ising model does not exhibit a phase transition for $T > 0$. On the other hand, the 2D Ising model solved by Onsager showed that in the absence of an external magnetic field there is a continuous phase transition for finite temperature [6].

3. Elementary theory of phase transitions

The most familiar examples of phase transitions are those involving water, either melting ice to water or its evaporation. These phase transitions, named first-order phase transitions, are characterized by having discontinuous values in their extensive variables[3]. However, there is a subtlety when water is transformed into a gas. If it is at a sufficiently high temperature and pressure, there is no transition between a liquid and a gas. The limiting pressure and temperature above which there is no phase transition are called the critical pressure and critical temperature, respectively.

At the critical pressure and temperature there is a continuous phase transition or second-order transition, and in this case the extensive variables of the system are continuous, while its first derivatives, such as the specific heat or isothermal compressibility, are discontinuous. It is important to mention that this kind of phase transition occurs for all pure substances, not

[3] The extensive variables of a thermodynamic system are its energy E, entropy S, volume V and particle number N. The fundamental relationships are given by the thermodynamic potentials such as $E = E(S, V, N)$ or the Helmholtz free energy $F = F(T, V, N)$ which are linked by Legendre transformations and the Euler relationship $E = TS - pV + \mu N$ that states the extensive behaviour of E, S, V and N.

only water, but carbon dioxide, gold and others. In a pressure–temperature phase diagram ($p - T$ diagram), this point is referred to as the critical point.

Second-order phase transitions are also seen in magnetic systems, such as the Curie point in ferromagnets which separates the paramagnetic phase from the ferromagnetic one. That means that below the Curie temperature, the system presents spontaneous magnetization in the absence of an external magnetic field, whereas above the Curie temperature the system is not magnetized and only responds when an external magnetic field is applied. It is our goal to illustrate what happens in second-order transitions and how the thermodynamic properties of the systems behave.

3.1. The order parameter and the correlation function

As stated above, in a second-order transition the first-order derivatives of the extensive variables of the system are discontinuous. These thermodynamic quantities, such as specific heat, isothermal compressibility or magnetic susceptibility in a magnetic system follow a power law near the transition.

For example,

$$C_H \sim |1 - T/T_c|^{-\alpha}, \tag{5a}$$

$$\chi_M \sim |1 - T/T_c|^{-\gamma}, \tag{5b}$$

where C_H and χ_M denote the specific heat and the susceptibility, respectively. T_c is the critical temperature, T is the current temperature of the system and α and γ are critical exponents.

The dimension of space is very important in phase transitions. Critical exponents fall into different universality classes depending upon both the space dimension and the degrees of freedom of the system. For example, the van der Waals' equation of state reproduces correctly the critical exponents of a real liquid–gas for a four-dimensional space.

Nonetheless, critical exponents give vital information about the thermodynamic system under study because they are linked with a key concept for understanding phase transitions, the order parameter. The relationship between the critical exponents and the order parameter is that the behaviour of the latter near T_c is usually described by the former. But what is the order parameter? In simple terms, the order parameter is the indicator of a phase transition.

For example, in a magnetic system, the magnetization $\mathbf{M}$ is the order parameter. Because in the absence of an external magnetic field, in the paramagnetic phase, the spins have equal probability of pointing in any direction, the net magnetic moment of the system vanishes and $\mathbf{M} = 0$. Below the critical temperature or Curie temperature, in the ferromagnetic phase, the spins tend to align in one direction, causing the net magnetic moment to be different from zero and $\mathbf{M} \neq 0$. On the other hand, for a van der Waals' fluid, the density is the order parameter and for the Bose–Einstein condensation it is the wavefunction itself, amongst other examples.

It is in the order parameter where spontaneous symmetry breaking is reflected. Considering the magnetic system, in the absence of an external magnetic field, the high-temperature phase (paramagnetic phase) exhibits an isotropic alignment of magnetic moments but the low-temperature phase (ferromagnetic phase) does not. This isotropy is broken ($\mathbf{M} \neq 0$), with a given preferential direction; this is called spontaneous symmetry breaking.

It is worth mentioning that, strictly speaking, one should consider the vector character of the order parameter; nevertheless its absolute value $M = |\mathbf{M}|$ also reflects the transition. If we consider its absolute value, we would not be able to determine the direction in which the system magnetizes, but this illustrates that the magnetization does not vanish below the critical temperature.

To really understand the behaviour of a system near a phase transition we need to look at its microscopic behaviour. Such information is enclosed in the correlation function $G(r, T)$, that expresses how the local order parameter at one position is correlated with itself a distance r away. The correlation function is explicitly written as $G(r, T)$ to indicate that it depends on both the temperature of the system T and the distance r.

Above the critical temperature, the correlation function falls off exponentially:

$$G(r, T) \sim \exp\left(-\frac{r}{\xi(T)}\right) \qquad (T > T_c), \tag{6}$$

where $\xi(T)$ is called the correlation length, which as indicated, depends on temperature.

At the transition, the correlation falls off as a power law given by:

$$G(r, T) \sim \frac{1}{r^{d-2+\eta}} \qquad (T = T_c), \tag{7}$$

where d is the dimension of space and η is a critical exponent. This power-law decrease of the correlation function at the critical point implies that there is no length scale in the system, and consequently far regions in the system are correlated.

Finally, below the critical temperature, the correlation function reaches a constant value for large r. Such ordering is called long-range order and is a consequence of cooperative effects that cause regions of space to be correlated with nearby regions, which in turn causes a farther region to be correlated. In this case, the deviation from the asymptotic value can be described by:

$$G(r, T) - G(\infty, T) \sim \exp\left(-\frac{r}{\xi(T)}\right) \qquad (T < T_c). \tag{8}$$

The correlation length also follows a power law as the transition is approached from either $T > T_c$ or $T < T_c$, given by:

$$\xi(T) \sim |1 - T/T_c|^{-\nu}, \tag{9}$$

ν being another critical exponent.

It is interesting to notice that the critical exponents are not independent of each other, because of the following scaling laws [14]:

$$\gamma = \nu(2 - \eta), \tag{10a}$$

$$2 = \alpha + 2\beta + \gamma, \tag{10b}$$

$$\nu d = 2 - \alpha, \tag{10c}$$

$$\gamma = \beta(\delta - 1), \tag{10d}$$

so it is only necessary to know two of them to determine the others.

3.2. The scaling hypothesis

The scaling hypothesis is, as its name indicates, a hypothesis. It does not rely on any model but has been very successful in correlating experimental data. The basic idea of the scaling hypothesis is that the long-range correlations around T_c are responsible for all singular behaviour [15].

So far, it seems that the important parameter in a phase transition is the order parameter, and for a long time it was considered that if there was no spontaneous symmetry breaking in

the order parameter in a system then that system does not exhibit a phase transition. This belief is false and a brief example will be discussed later (see section 8).

In the scaling hypothesis, instead of looking at the order parameter, we focus our attention on a quantity we briefly mentioned in section 3.1: the correlation length ξ. It states that the divergence of ξ near T_c is responsible for the singular dependence on $1 - T/T_c$ of physical quantities, and, as far as the singular dependence is concerned, ξ is the only relevant length in the system [15].

It is not the scope of this paper to derive the scaling laws, nor to prove them by renormalization theory, but just to present the importance of the scaling hypothesis. An extensive discussion of the scaling hypothesis and renormalization theory can be found in [15, 16].

4. Mean-field and Onsager's solution

From statistical mechanics we know that,

$$Z = \mathrm{Tr}\,(\mathrm{e}^{-\mathcal{H}/k_\mathrm{B}T}), \tag{11a}$$

$$\langle \mathbf{m} \rangle = \frac{1}{Z}\,\mathrm{Tr}\,(\mathbf{m}\mathrm{e}^{-\mathcal{H}/k_\mathrm{B}T}), \tag{11b}$$

where $\mathbf{m} = \mathbf{M}/N$. The mean-field solution considers that $\mathbf{s}_i = \mathbf{m} + \Delta\mathbf{s}_i$ with $\Delta s_i \ll m$, implying that fluctuations in magnetization are small compared with the magnetization. In that sense, a mean-field model considers that if a spin is chosen in the lattice it is affected by its neighbours, but they are not affected by its presence [17].

Considering the mean field model for first corrections only and in absence of an external magnetic field, the Hamiltonian is,

$$\mathcal{H} = -\frac{J}{2}\sum_{\langle ij \rangle}(m^2 + 2\mathbf{m}\cdot\Delta\mathbf{s}_i), \tag{12}$$

that simplifies to,

$$\mathcal{H} = \frac{1}{2}JzNm^2 - Jz\mathbf{m}\cdot\sum_i \mathbf{s}_i, \tag{13}$$

where z is the number of nearest neighbours (in the 2D case $z = 4$). That way the partition function is simply,

$$Z = \mathrm{Tr}\left[\exp\left(-\frac{JzN}{2k_\mathrm{B}T}m^2 + \frac{Jz}{k_\mathrm{B}T}\mathbf{m}\cdot\sum_i \mathbf{s}_i\right)\right], \tag{14}$$

so,

$$Z = \exp\left(-\frac{JzN}{2k_\mathrm{B}T}m^2\right)\prod_{i=1}^{N}\sum_{s_i=-1}^{1}\exp\left(\frac{Jzms_i}{k_\mathrm{B}T}\right), \tag{15}$$

where $s_i = \pm 1$ denotes the two possible values of a spin in the Ising model. Finally, Z is given by,

$$Z = \exp\left(-\frac{JzN}{2k_\mathrm{B}T}m^2 + N\ln\left[2\cosh\left(\frac{Jzm}{k_\mathrm{B}T}\right)\right]\right), \tag{16}$$

and the Landau free energy [17–20] is related to the partition function as $F_{\mathrm{L}} = -k_{\mathrm{B}}T \ln Z$, hence,

$$F_{\mathrm{L}} = \frac{1}{2} JzNm^2 - Nk_{\mathrm{B}}T \ln\left[2\cosh\left(\frac{Jmz}{k_{\mathrm{B}}T}\right)\right]. \tag{17}$$

Doing a Taylor expansion of $\ln(\cosh x) = (1/2)x^2 - (1/12)x^4 + \mathcal{O}(x^6)$, the Landau free energy may be written as,

$$F_{\mathrm{L}} \approx -Nk_{\mathrm{B}}T \ln 2 + \left(\frac{1}{2}JzN - \frac{NJ^2z^2}{2k_{\mathrm{B}}T}\right)m^2 + \frac{NJ^4z^4}{12(k_{\mathrm{B}}T)^3}m^4 + \mathcal{O}(m^6). \tag{18}$$

The first term only depends on the temperature, not the magnetization, and will be identified as F_o. The second term is quadratic in m and its coefficient will be identified as $a(T)/2$, while the last term is quartic in m and its coefficient will be identified as $b(T)/4$,

$$F_{\mathrm{L}} \approx F_o + \frac{1}{2}a(T)Nm^2 + \frac{1}{4}b(T)Nm^4. \tag{19}$$

Under this proposal, if $a(T)$ and $b(T)$ are both positive, only $m = 0$ is a minimum. On the other hand if $b(T)$ is positive and $a(T)$ changes sign, then $m = 0$ is a local maximum and the minimum of F_{L} occurs at $m \neq 0$, that is an indicator of a phase transition. The transition takes place at the critical temperature T_{c}, which is determined when $a(T)$ changes sign, i.e. $a(T_{\mathrm{c}}) = 0$. As a result, T_{c} for the Ising model is,

$$k_{\mathrm{B}}T_{\mathrm{c}} = zJ, \tag{20}$$

so for the 2D case $k_{\mathrm{B}}T_{\mathrm{c}} = 4J$.

Near the critical temperature, the coefficients for the Landau free energy are,

$$a(T) \approx k_{\mathrm{B}}(T - T_{\mathrm{c}}), \tag{21a}$$

$$b(T) \approx \frac{1}{3}k_{\mathrm{B}}T_{\mathrm{c}}. \tag{21b}$$

The minima of F_{L} are,

$$M/N = 0 \qquad T \geqslant T_{\mathrm{c}}, \tag{22a}$$

$$M/N = \pm\left(3\frac{T_{\mathrm{c}} - T}{T_{\mathrm{c}}}\right)^{1/2} \qquad T < T_{\mathrm{c}}, \tag{22b}$$

which in turn provides the first mean-field critical exponent $\beta = 1/2$.

Considering $H \neq 0$, it is straightforward to prove that,

$$F_{\mathrm{L}} = \frac{1}{2}JzNm^2 - Nk_{\mathrm{B}}T \ln\left[2\cosh\left(\frac{Jmz + H}{k_{\mathrm{B}}T}\right)\right], \tag{23}$$

and minimizing it with respect to m, the next transcendental equation is found,

$$m = \tanh(\beta(Jmz + H), \tag{24}$$

doing a Taylor expansion of $\tanh^{-1}(x) = x + (1/3)x^3 + \mathcal{O}(x^5)$, and rearranging terms,

$$H = m(T - T_{\mathrm{c}}) + \frac{1}{3}m^3T, \tag{25}$$

which at the critical temperature becomes,

$$H = \frac{k_B T_c}{3} m^3, \tag{26}$$

showing that the second mean-field critical exponent is $\delta = 3$,

$$H \sim M^{\delta}, \tag{27}$$

when $T = T_c$.

Although it is not within the scope of this paper to present the exact solution, some important results that will be used in section 6 are given here. The magnetization is found to be,

$$M/N = 0 \qquad T > T_c, \tag{28a}$$

$$M/N = \pm[1 - \sinh^{-4}(2\beta J)]^{1/8} \qquad T < T_c, \tag{28b}$$

which only holds in the thermodynamic limit ($N \to \infty$ and $V \to \infty$, but N/V constant). The critical temperature is,

$$k_B T_c = \frac{2J}{\ln(1 + \sqrt{2})} \approx 2.269J. \tag{29}$$

Also, near T_c the heat capacity behaves as,

$$C_H = N k_B \frac{2}{\pi}\left(\frac{2J}{k_B T_c}\right)^2\left[-\ln\left(1 - \frac{T}{T_c}\right) + \ln\left(\frac{k_B T_c}{2J}\right) - \left(1 + \frac{\pi}{4}\right)\right], \tag{30}$$

so C_H diverges logarithmically near the transition. From the results above, the critical exponents $\beta = 1/8$ and $\alpha = 0$ are found. All the critical exponents found in the mean-field and the exact solution are presented in table 1 and section 6. A complete discussion on the exact solution can be found in [14, 19, 20].

5. Numerical solution

5.1. The Metropolis–Hastings algorithm

In principle we could construct all the possible states the system can access $\{n\}$ and their energies $E_{\{n\}}$. With that information, we could construct the partition function and recover all the thermodynamics of the system. However, there are 2^N possible states the system can access, so it is impractical to follow this path for large systems that obey $N \gg 1$. This problem is solved by designing a Markov chain (or transition matrix) in such a way that its stationary distribution is the desired distribution, in this case,

$$P(\{n\}) = \frac{1}{Z} e^{-E_{\{n\}}/k_B T}, \tag{31}$$

where $\{n\}$ is a possible state of the system and $P(\{n)$ is its stationary distribution.

But what is a Markov chain? It is one type of stochastic process. It is an evolution in time that is not determinist, but there is a transition probability from the current state to a new state. A Markov chain satisfies that the probability distribution of the next state depends only on the current state.

If an initial probability distribution is given by $\mathbf{P}(t = 0) = \mathbf{P}_0$ and $\mathcal{P}$ is the transition matrix at one step, it is easy to prove that the probability distribution at the nth step is simply,

$$\mathbf{P}_n = (\mathcal{P}^N)^{\mathrm{T}}\mathbf{P}_0, \tag{32}$$

where the probability distributions are written as column vectors and the superscript T denotes transposition.

It is our interest to know if there is a stationary distribution $\mathbf{P}_\infty$, i.e. if the next limit exists,

$$\mathbf{P}_\infty = \lim_{t\to\infty} (\mathcal{P}^{\mathrm{T}}\mathbf{P}_0). \tag{33}$$

Because $\mathbf{P}_0$ is the initial distribution and does not depend on t, the problem reduces to determining if $\lim_{t\to\infty}\mathcal{P}^{\mathrm{T}}$ exists. It is straightforward to prove that if $\mathbf{P}_\infty$ exists and $\mathbf{P}_0 = \mathbf{P}_\infty$, then $\forall\ t$, $\mathbf{P}_t = \mathbf{P}_\infty$.

A matrix is called ergodic if it is possible to go from every state to every other state (not necessarily in one move). This condition can be rewritten the following way: a matrix is ergodic, i.e. $\lim_{t\to\infty}\mathcal{P}^{\mathrm{T}}$ exists, if and only if its only unitary eigenvalue is 1. If the multiplicity of the eigenvalue is m, the theorem also holds. This condition is written as,

$$\mathbf{P} = \mathcal{P}^{\mathrm{T}}\mathbf{P}, \tag{34}$$

that expressed in index notation and using the fact that for a Markov chain $\sum_i \mathcal{P}_{ij} = 1$, where $\mathcal{P}_{ij}$ is the transition probability from state i to state j, is:

$$\sum_{j\neq i} P_i\,\mathcal{P}_{ij} = \sum_{j\neq i} P_j\,\mathcal{P}_{ji}. \tag{35}$$

This equality is known as the global balance equation. However, if it is possible to find a stationary distribution that for all pair of states i and j,

$$P_i\,\mathcal{P}_{ij} = P_j\,\mathcal{P}_{ji}, \tag{36}$$

then the global balance equation will trivially hold. This condition is named the detailed balance equation and is the basis of the Metropolis–Hastings algorithm.

In statistical mechanics, in the canonical ensemble, the stationary distribution is know and is given by the density matrix, so the probability that the system is in a state $\{n\}$ is given by equation (31). In that sense, in order to design a Markov chain that respects the desired distribution it is only necessary to consider the detailed balance equation (36), that may be rewritten in a more enlightening manner as,

$$\frac{P(\{n\})}{P(\{m\})} = \frac{\mathcal{P}(\{m\}\to\{n\})}{\mathcal{P}(\{n\}\to\{m\})}. \tag{37}$$

And because of (31), this condition is simply,

$$\frac{P(\{n\})}{P(\{m\})} = \exp(-[E(\{n\}) - E(\{m\})]/k_{\mathrm{B}}T), \tag{38}$$

so there is no need to calculate the partition function.

The Metropolis–Hastings algorithm works as follows [21, 22]:

(i) The system is at state $\{m\}$ and the new configuration $\{n\}$ is proposed with probability $g(\{m\}\to\{n)$.

(ii) After this new state is proposed, it will accepted with probability $\alpha(\{m\}\to\{n)$ or rejected with probability $1-\alpha(\{m\}\to\{n)$. That way, the transition probability $\mathcal{P}(\{m\}\to\{n)$ simply becomes,

$$\mathcal{P}(\{m\}\to\{n) = g(\{m\}\to\{n)\alpha(\{m\}\to\{n). \tag{39}$$

(iii) The detailed balance equation is written as,

$$\frac{P(\{n)}{P(\{m)} = \frac{g(\{m\} \to \{n)\alpha(\{m\} \to \{n)}{g(\{n\} \to \{m)\alpha(\{n\} \to \{m)}, \tag{40}$$

so,

$$\frac{\alpha(\{m\} \to \{n)}{\alpha(\{n\} \to \{m)} = \frac{P(\{n)}{P(\{m)}\frac{g(\{n\} \to \{m)}{g(\{m\} \to \{n)}, \tag{41}$$

(iv) In order to fulfil the detailed balance equation, the rate of acceptance may be expressed as,

$$\alpha(\{m\} \to \{n) = \min\left(1, \frac{P(\{n)}{P(\{m)}\frac{g(\{n\} \to \{m)}{g(\{m\} \to \{n)}\right). \tag{42}$$

In the Ising model when $\{n\}$ and $\{m\}$ only differ by one spin, $g(\{n\} \to \{m) = g(\{m\} \to \{n)$, so the rate of acceptance is,

$$\alpha(\{m\} \to \{n\}) = \min(1, \exp[-\Delta E(\{n\}, \{m\})]/k_{\mathrm{B}}T). \tag{43}$$

Before discussing the algorithm in detail it must be pointed out that it is sufficient to satisfy the principle of detailed balance. One could select the Metropolis–Hastings rate or the Glauber rate and have the same equilibrium results [23].

With those ideas in mind, the Metropolis–Hastings algorithm for the Ising model is as follows. First, a $L \times L$ square lattice is created and in every site of the lattice a spin is set with equal probability of it being ± 1 (see section 5.4).

Each step of the algorithm is:

(i) Choose at random one site k in the lattice.
(ii) Calculate the energy difference ΔE_k between the actual energy and the energy if the spin is flipped.
(iii) If $\Delta E_k < 0$, we accept the new configuration. If not, we accept it with probability $\exp(-\Delta E_k/k_{\mathrm{B}}T)$.
(iv) The energy and magnetization of the system are saved.

The Metropolis–Hastings algorithm samples states according to the appropriate probability distribution and then temporal sequences of energies and magnetizations (generated by the sampling process) are averaged and observables calculated. It is important to emphasize that the algorithm only generates configurations in agreement with the probability distribution; it does not compute thermodynamic quantities, but only samples ensembles from which thermodynamic quantities must be determined. In the next sections, techniques for recovering those quantities are discussed.

Before presenting those techniques, it is necessary to define a Monte Carlo step (MC step) as the product $N = L^2$ with the number of steps in the algorithm. For example, for a system with a lattice size $L = 50$, a MC step is 2500 steps of the algorithm. That way a MC step takes into account the lattice size, while a step of the algorithm does not. In that sense, performing 1000 MC steps for different lattices sizes allows the same sampling in all the lattices, whereas performing 1000 steps of the algorithm for different lattices sizes does not. It is natural that the following question arises: How many MC steps produce a good sampling?

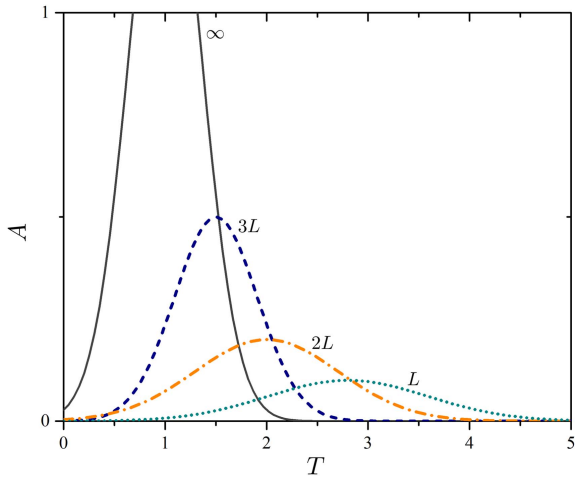

Figure 1. Typical behaviour of a physical quantity A versus temperature close to the critical point for various system sizes.

This question is not so easy to answer because it depends on the temperature of the system, as will be clear later in section 6. Nevertheless, if, while computing observables such as energy and magnetization, the curves are noisy, then it is necessary to perform more MC steps.

5.2. Finite size scaling

So far we have presented the mean-field, the Onsager and the numerical solutions. However, one problem arises in the numerical solution: while the mean-field and the exact solutions are in the thermodynamic limit ($N \to \infty$ and $V \to \infty$, but N/V constant), in the numerical solution it is impossible to achieve N, $V \to \infty$. Although we are incapable of achieving the thermodynamic limit a numerical computation, *K*. Binder developed the finite-size scaling technique for analysing finite-size systems such as the ones considered in computational simulations [24–26].

As we have stated before, near the critical temperature, the correlation length diverges following a power law (9),

$$\xi \sim |1 - T/T_c|^{-\nu}. \tag{44}$$

For a finite system, the thermodynamics quantities are smooth functions of the system parameters, so divergences of the critical point phenomena are absent. Despite this fact, in the scaling region ($\xi \gg L$), we can see traces of these divergences in the occurrence of peaks: peaks become higher and narrower and their location is shifted with respect to the location of the critical point as the system size increases (see figure 1). These characteristics of peak shape as a function of temperature are described in terms of the so-called finite-size scaling exponents [8]:

- The shift in the position of the maximum with respect to the critical temperature is described by,

$$T_c(L) - T_c(\infty) \propto L^{-\lambda} \tag{45}$$

- The width of the peak scales as,

$$\Delta T(L) \propto L^{-\Theta} \tag{46}$$

- The peak height grows with the system size as,

$$A_{\max}(L) \propto L^{\sigma_{\max}}. \tag{47}$$

Defining $t = |1 - T/T_c|$, the finite-size scaling ansatz is formulated as follows [8]:

$$\frac{A_L(t)}{A_\infty(t)} = f\left[\frac{L}{\xi_\infty(t)}\right], \tag{48}$$

where A is a physical quantity. Assuming that the exponent of the critical divergence of A is σ, and using the fact that $\xi \sim t^{-\nu}$, the scaling ansatz is formulated as,

$$A_L(t) = t^{-\sigma} f[Lt^{-\nu}], \tag{49}$$

which can be rewritten as,

$$A_L(t) = L^{\sigma/\nu}\phi[L^{1/\nu}t], \tag{50}$$

where the scaling function f is replaced by ϕ, by extracting the factor $(Lt^\nu)^{\sigma/\nu}$ from f and writing the remaining function in terms of $(Lt^\nu)^{1/\nu}$. From (50) it is clear that [8]:

- The peak height scales as $L^{\sigma/\nu}$, hence $\sigma_{\max} = \sigma/\nu$.
- The peak position scales as $L^{-1/\nu}$, hence $\lambda = 1/\nu$.
- The peak width also scales as $L^{-1/\nu}$, hence $\Theta = 1/\nu$.

These are the finite-size scaling laws for any thermodynamic quantity which diverges at the critical point as a power law. From these laws it is clear that if the peak height, position and width are calculated as a function of the system size, the critical exponents ν and σ can be determined.

Nevertheless, the finite-size scaling technique presents difficulties due a to a phenomenon called critical slowing-down [3, 8–10]. Because of critical slowing-down configurations change very slowly, and it is difficult to sample enough configurations. Near the critical point, the fluctuations increase and the time needed to obtain reliable values for the quantities measured also increases. As the system size increases, calculations for larger systems require more time, not only because of the computational effort needed per MC step for a larger system, but also because we need to generate more and more configurations in order to obtain reliable results.

5.3. The correlation function

In systems where a physical magnitude relies on position, one generally asks, given a measure at point $\mathbf{r}_i$, what is the relation between another measure at a position $\mathbf{r}_j$? This is given by the spatial correlation function, and if the system presents translational and rotational symmetry (such as the Ising model) the correlation function does not depend on the absolute positions, but on the distance between them $r = |\mathbf{r}_i - \mathbf{r}_j|$. The correlation function we are interested in is the spin–spin correlation function that is given by,

$$G(r, T) = \langle s(0)s(r)\rangle - \langle s(0)\rangle^2, \tag{51}$$

where $\langle s(0)\rangle = \langle s(r)\rangle = M/N$ is the magnetization per site. Because of the fact that, for a given temperature, M reaches a constant value, the behaviour of the correlation function is carried by the first term of (51). Thus we will consider the correlation function only as,

$$G(r, T) = \langle s(0)s(r)\rangle. \tag{52}$$

We are limited to obtaining the correlation function up to $L/2$, where L is the lattice size. This comes as a price of the periodic boundary conditions we are using. For example, if we were to calculate the correlation function up to the value $r = L$ we would find that the correlation function would be equal to 1 there, which is wrong because we would be computing the correlation function at $r = 0$.

The process for numerically computing the correlation function is the following: for each spin in the lattice, we determine the value of the local correlation function in $r = n$ taking the average magnetic state of the nearest neighbours found advancing n steps in one direction (not mixing $\hat{e}_i$ with $\hat{e}_j$, i.e. not moving in diagonals). The global correlation function is taken as the average of all the local correlation functions. The process is repeated for multiple simulations of the Ising model.

5.4. Hints, tips and improvements to the algorithm

As soon as Monte Carlo methods are used, one has to think on ways of making efficient calculations, as the brute force involved in a Monte Carlo simulation often requires many trials to reduce standard deviation.

- Although periodic boundary conditions are the most common boundary conditions used, they are not the only choice. Another one is to used fixed boundary conditions, which would mean adding an extra layer of spins in the lattice all pointing in one fixed direction, meaning that every spin in the real lattice that is at its boundaries interacts with a fixed direction. Nevertheless, usually periodic boundary conditions are easier to implement and are closer to the way of thought used to find the exact solutions.
- Due to the fact that the interaction is between nearest neighbours, the energy differences can be easily calculated and the exponentials $\exp(-\Delta E_k/k_{\mathrm{B}}T)$ (used to calculate acceptance probabilities) stored in a list, thus avoiding calculation of the exponentials in every step of the algorithm.
- It is not necessary that the initial configuration is always random—one could start from some other initial configuration. The reader can observe the dynamic of the system by choosing different initial configurations for a given temperature and determine which ones converge faster.
- Monte Carlo methods are always good candidates for parallelization, which even in a dual-core CPU will halve the calculation time.
- One can remove some ‘randomness’ from the method to improve efficiency. In the case of the Ising model, we know that the system will have preferred states as a function of the temperature. For temperatures below the critical temperature, once the system is near a local energy-minimum, it will hardly jump to another one (even if the energy gap is huge). All annealing methods are prone to this phenomenon, and hence once the standard deviations of the last steps start to decrease, the system should be randomized entirely to make sure one is not just sampling a single region of the entire space of states.
- One can also improve the selection of spins to flip, and change a completely uniform random distribution to a random walker (or walkers) that moves through the lattice.

However, there are some considerations when doing this because one might actually modify the result or slow down the convergence rate. The step size is crucial to ensure a good convergence ratio. What could we say about the walker if the last 10 attempts to switch a spin have failed? Well, the zone it is moving through is already in a stable position, hence it seems wise to increase the step size of the random walker. So the goal is to accelerate the relaxation process by trying to modify spins in unstable areas (which we assume are stable because a lot of changes are accepted). The best results are achieved if one monitors the standard deviation of the system in order to restart it as soon as it falls in a stable position.

- It is important to perform simulations with a good random number generator. This is usually not a problem with most computational languages, but it is something to take into account because a poor random generator will be unable to sample enough configurations, thus obtaining unreliable results.

6. Numerical results

Energy, magnetization, specific heat and magnetic susceptibility are studied first. It is a simple exercise to show that the specific heat C_H and the magnetic susceptibility χ_M can be expressed in terms of the fluctuations of the extensive variables,

$$C_H = \left(\frac{\partial E}{\partial T}\right)_H = \frac{1}{k_B T^2}(\langle E^2\rangle - \langle E\rangle^2), \tag{53a}$$

$$\chi_M = \left(\frac{\partial M}{\partial H}\right)_T = \frac{1}{k_B T}(\langle M^2\rangle - \langle M\rangle^2). \tag{53b}$$

For a system in the thermodynamic limit, below the critical temperature, the system has equal probability of magnetizing with a positive value of M or its negative value. Nevertheless, in the absence of an external magnetic field there is no chance for the system to go from the positive branch of spontaneous magnetization to the negative one and vice versa. However, for finite size systems there is a characteristic time (that depends of course on the lattice size) in which the system can go from one branch of spontaneous magnetization to the other. Simply averaging the magnetization would yield an incorrect value, for this reason: instead of using $\langle M\rangle$ as the order parameter, $\langle|M|\rangle$ will be used [10]. If $\langle|M|\rangle$ is considered as the order parameter, χ_M is also calculated using $\langle|M|\rangle$ instead of $\langle M\rangle$, so the susceptibility we compute is not exactly the 'true' one. However, in the $T < T_c$ region they are equal and in the $T > T_c$ region they only differ by a constant, so the critical exponents are equal. Likewise, this consideration also 'smooths' the computation of thermodynamic quantities that are derivatives of the order parameter, and in general of any physical quantity that presents a peak.

Because magnetization M, energy E, specific heat C_H and magnetic susceptibility χ_M are extensive variables, intensive ones were constructed by dividing them by the number of sites in the lattice $N = L^2$. From now on, M will refer to magnetization per site, E energy per site, C_H specific heat per site and χ_M magnetic susceptibility per site. All simulations were performed considering $k_B = 1$ and $J = 1$. In figures 2–4, magnetization per site M, magnetic susceptibility per site χ_M and specific heat per site C_H as functions of the temperature T are presented. This plots were constructed by performing 15 000 MC steps per lattice size L.

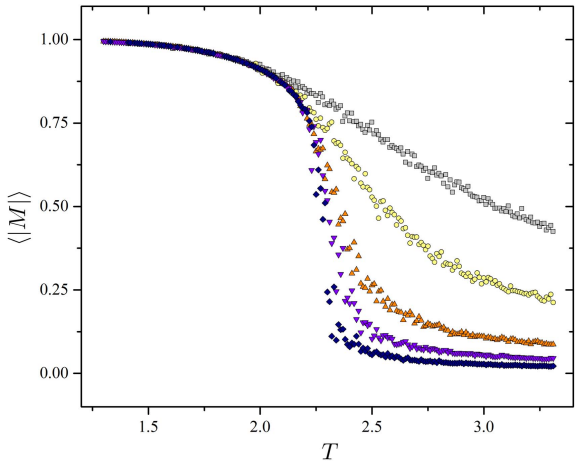

Figure 2. Magnetization per site M versus temperature T for different lattice sizes $L = 5$ (squares), 10 (circles), 25 (up triangles), 50 (down triangles) and 100 (diamonds) for the 2D Ising model.

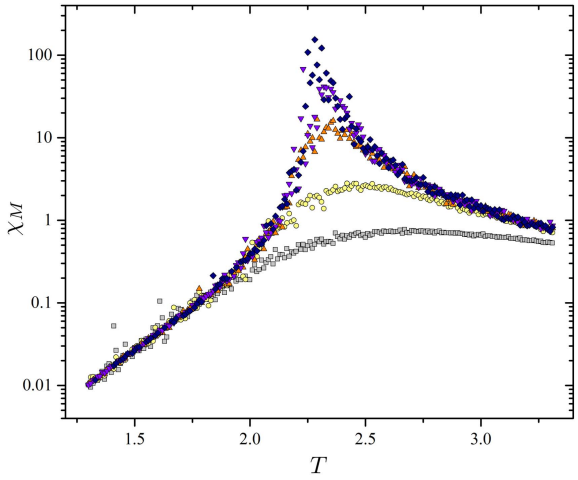

Figure 3. Magnetic susceptibility per site χ_M versus temperature T for different lattice sizes $L = 5$ (squares), 10 (circles), 25 (up triangles), 50 (down triangles) and 100 (diamonds) for the 2D Ising model.

6.1. How does the algorithm work?

In figures 5 and 6 simulations for a $L = 50$ lattice are presented. In figure 5 the behaviour of the order parameter is presented as a function of the 15 000 MC steps performed, while in figure 6 it is presented as a function of the energy of the system.

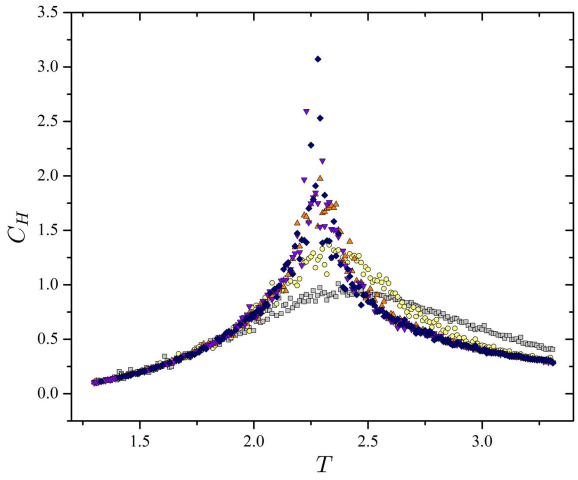

Figure 4. Specific heat per site C_H versus temperature T for different lattice sizes $L = 5$ (squares), 10 (circles), 25 (up triangles), 50 (down triangles) and 100 (diamonds) for the 2D Ising model.

From these figures important information is inferred. From figure 5 is clear that for $T < T_c$ and $T > T_c$ the behaviour of the system is relatively simple. In the ferromagnetic phase the magnetization settles around a value $M \neq 0$, while in the paramagnetic phase the order parameter settles around $M = 0$. But near the transition $T \approx T_c$, the system behaves exotically, the fluctuations in the order parameter are huge; M does not settle around a concrete value, but covers a broad range of values.

These observations are supported by figure 6, where it is clear that the algorithm samples states according to the probability distribution (see (31)).

- For $T < T_c$, there are few possible states to be sampled, but they are distributed in the phase space. This is due to the fact that states are sampled until the system magnetization reaches its final value. As the system gets magnetized, fewer and fewer states are accessible, because the acceptance probability gets smaller and smaller because $\Delta E_k < 0$ only if spins are flipped in the same direction of M and $\exp(-\beta \Delta E_k)$ is very small, so flipping a spin in the opposite direction of M is extremely improbable.
- For $T > T_c$ there are more possible states to be sampled, but they localized near $M = 0$. This is obvious from the fact that the system is in its paramagnetic phase and fluctuations are only caused by thermal effects.
- Near T_c, the simulation samples a broad portion of the phase space. Near the scaling region the generation of statistically independent configurations consumes more computational time due to the critical slowing-down. This fact implies that near the transition configurations change very slowly and correlate over large time scales. For this reason, near the critical temperature more MC steps are needed than for $T < T_c$ and $T > T_c$.

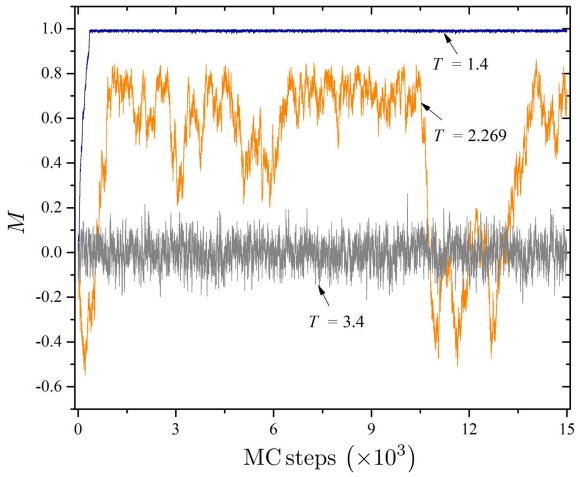

Figure 5. Magnetization per site M versus MC steps for temperatures $T = 1.4$, 2.269 and 3.4 for a lattice size of $L = 50$.

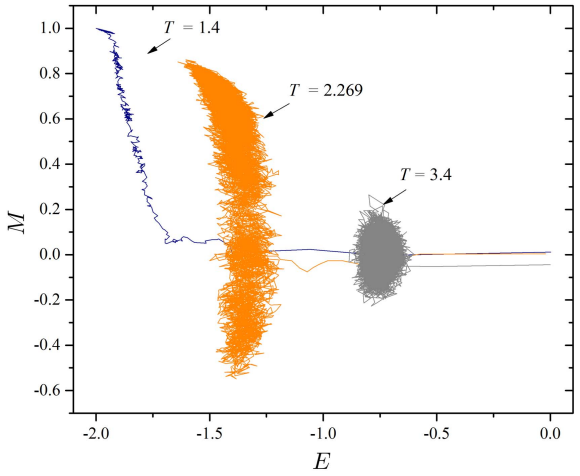

Figure 6. Magnetization per site M versus energy per site E for temperatures $T = 1.4$, 2.269 and 3.4 for a lattice size of $L = 50$.

6.2. Critical exponents and the correlation function

Despite the fact that for to correctly determine the critical exponents, finite-size scaling techniques must be used and the correlation function studied, in the 2D Ising model there is an analytical solution. For this reason, we consider it important to prove that our numerical

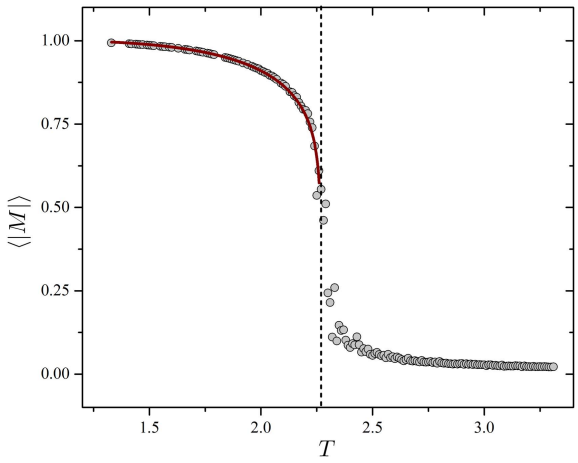

Figure 7. Magnetization per site M versus temperature T for a lattice size of $L = 100$ for the 2D Ising model. The curve in the left region was fitted with (54), where $A = 1.020 \pm 0.026$, $B = 1.027 \pm 0.017$ and $C = 0.129 \pm 0.007$.

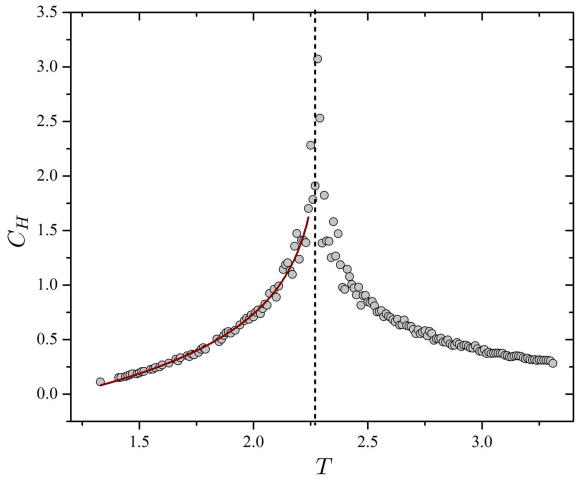

Figure 8. Specific heat per site C_H versus temperature T for a lattice size of $L = 100$ for the 2D Ising model. The curve in the left region was fitted with (55), where $A = -0.404 \pm 0.030$, $B = 1.293 \pm 0.059$ and $C = 2.303 \pm 0.011$.

solution is consistent with the analytical solution, hence figures 7 and 8 are fitted with Onsager's solution. The solution found by Onsager for the magnetization in the 2D Ising model is given by (28*a*), hence the curve used to fit the data presented in figure 7 in the $T < T_c$ regime is,

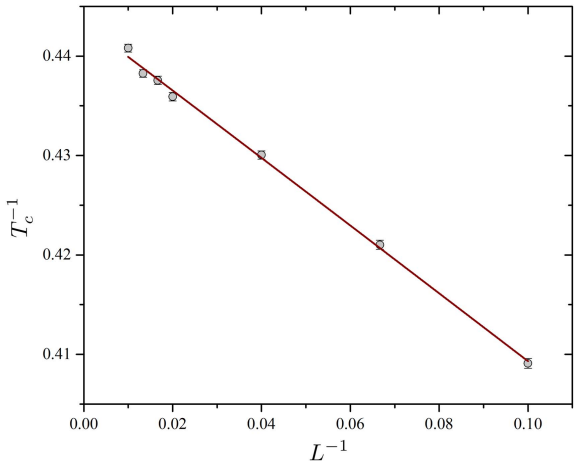

Figure 9. Inverse of the critical temperature T_c^{-1} versus inverse of lattice size L^{-1} for the 2D Ising model. The curve was fitted with a power law $T_c^{-1} = T_{c_\infty}^{-1} - bL^{-1/\nu}$, and the critical exponent ν was determined.

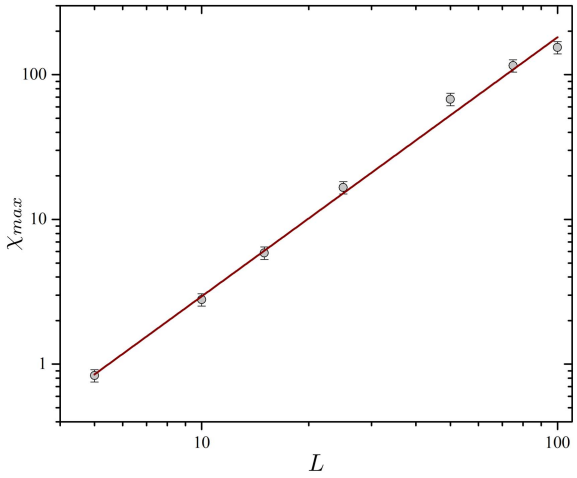

Figure 10. Peak height of the magnetic susceptibility $\chi_{\max}$ versus lattice size L for the 2D Ising model. The curve was fitted with a power law $\chi_{\max} = aL^{\gamma/\nu}$, and the critical exponent γ was determined.

$$M = \left[A - B\sinh^{-4}\left(\frac{2}{T}\right)\right]^{C}. \tag{54}$$

On the other hand, C_H is given by (30), so the curve used to fit the data presented in figure 8 in the $T < T_c$ regime is,

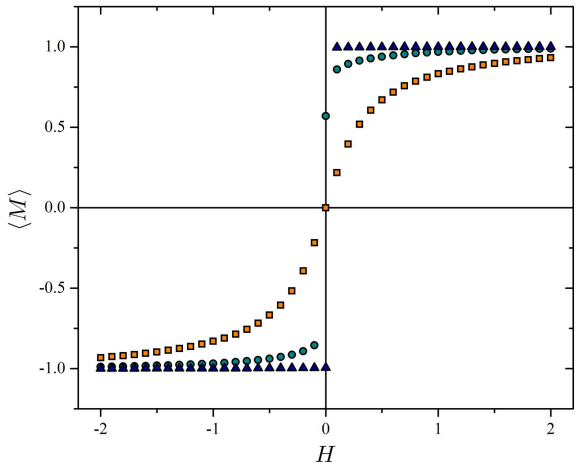

Figure 11. Magnetization per site M versus external magnetic field H for temperatures $T = 1.3$ (triangles), 2.269 (circles) and 3.3 (squares) for a lattice size of $L = 50$.

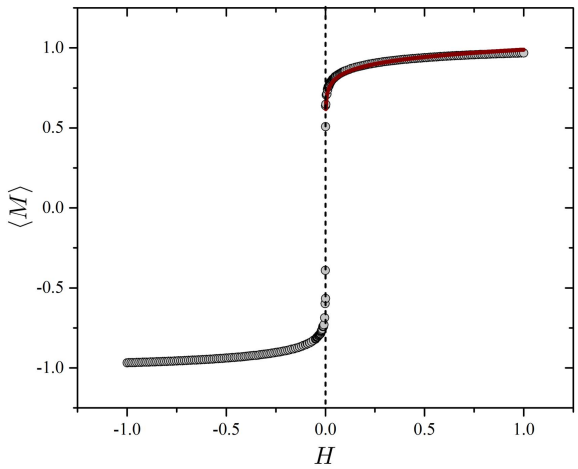

Figure 12. Magnetization per site M versus external magnetic field H for a lattice size of $L = 100$ at the critical temperature. The curve was fitted with a power law $M = aH^{1/\delta}$, and the critical exponent δ was determined.

$$C_H = A - B \ln\left(1 - \frac{T}{C}\right). \tag{55}$$

It is worth noticing the importance of considering large systems in order to obtain reliable results of the thermodynamic quantities because Onsager's solution is in the thermodynamic limit while numerical simulations are finite. In this manner, large systems were considered in

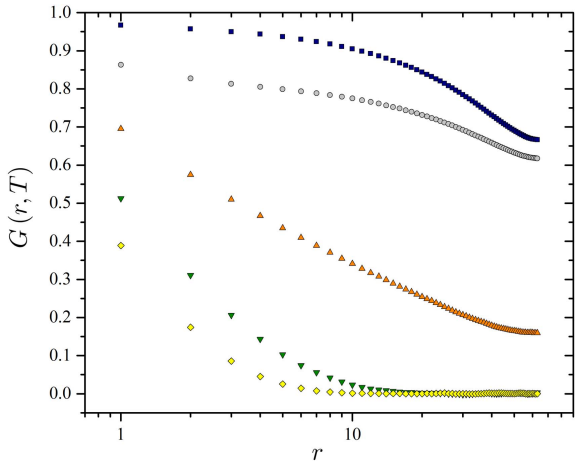

Figure 13. Correlation function $G(r, T)$ for temperatures $T = 1.5$ (squares), 2.0 (circles), 2.269 (up triangles), 2.6 (down triangles) and 3.1 (diamonds) for a lattice size of $L = 128$.

order to ensure the correct behaviour of magnetization and specific heat and from figures 7 and 8 the critical exponents β and α are determined.

To determine ν and γ, figures 9 and 10 were constructed in order to use finite size-scaling techniques. In figure 9 the critical temperature as a function of the lattice size $T_c(L)$ is obtained from figure 2 by finding the inflection point in each curve. In order to construct figure 10, 50 simulations of 15 000 MC steps each were performed for every lattice size considered and the peak height of the magnetic susceptibility χ_{max} was registered for every repetition. These values were averaged and presented with its standard deviation of the mean. We know that near the critical temperature T_c fluctuations are large, so the standard deviation of χ_{max} will be large too, but we are only interested in knowing how precise its mean is, that is why the standard deviation of the mean is used as a measure of uncertainty.

In figure 11 we plot the magnetization M as a function of the external magnetic field H for different temperatures, and from figure 12 the critical exponent δ is determined. These plots were also constructed by performing 15 000 MC steps per lattice size L. Later, in figure 13 the correlation function $G(r, T)$ is presented as a function of r for different temperatures. The behaviour discussed in section 3.1 is clearly observed in this figure. For $T > T_c$ the correlation function falls of exponentially, at $T = T_c$ if follows a power law and for $T < T_c$, it reaches a constant value for large r. Likewise, in figure 14 the correlation function at the critical temperature $G(r, T_c)$ is presented as a function of r. The critical exponent η is determined by fitting the data with the curve,

$$G(r, T_c) = A\frac{\exp(-r/B)}{r^C}. \tag{56}$$

These plots were constructed by performing 100 simulations of 15 000 MC steps each, for every temperature considered and the correlation function was registered for every repetition and then averaged.

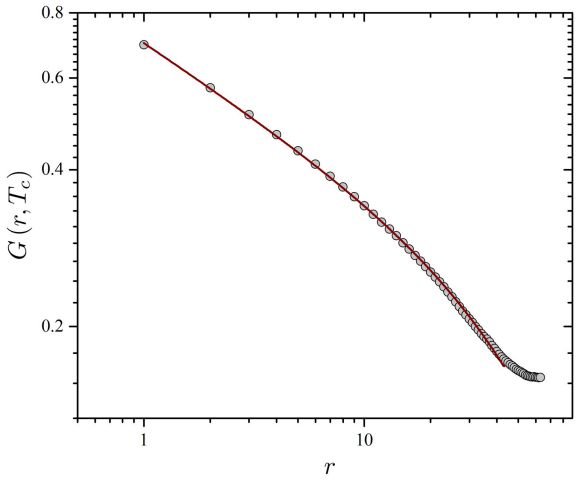

Figure 14. Correlation function $G(r, T)$ at the critical temperature T_c for a lattice size of $L = 128$. The curve was fitted with (56), where $A = 0.706 \pm 0.002$, $B = 108.525 \pm 2.752$ and $C = 0.277 \pm 0.002$.

Table 1. Critical exponents and critical temperature of the 2D Ising model given by Onsager, the mean-field and the numerical solutions.

Exponent	Onsager	Mean-field	Numerical
α	0	0	0
β	0.125	0.5	0.129 ± 0.007
γ	1.750	1	1.779 ± 0.225
ν	1	0.5	0.994 ± 0.098
η	0.250	0	0.277 ± 0.002
δ	15	3	14.641 ± 0.821
T_c	2.269	4	2.269 ± 0.002

Finally, in table 1, the critical exponents for the 2D Ising model are presented as found by Onsager along with the mean-field and numerical solutions.

7. Discussion

From table 1 is clear that the mean-field solution is inconsistent with the Onsager solution. Why is the mean-field solution not consistent? In its derivation, fluctuations in the order parameter are neglected. However, in the scaling region, these fluctuations are of great relevance to the thermodynamic quantities, so neglecting them will of course generate incorrect results in this region, such as the critical temperature and the critical exponents.

The main problem with most of the mean-field solutions is that the Landau free energy coefficients are expanded in Taylor series around T_c. This expansion presupposes that the coefficients are analytical around T_c, a supposition that is not valid. It is also worth to notice

that the mean-field model presented here gives the same critical exponents for any dimension. This of course is a severe problem, because universality classes depend on both the space dimension and the system degrees of freedom. Although most of the mean-field models do not reproduce correctly the critical exponents, they provide a useful insight to phase transitions, so they should not be discarded. Actually mean-field models such as the Ginzburg–Landau model, are used to describe phenomena such as superfluidity and superconductivity (see for example Annett's book [27]). On the other hand, the numerical results are consistent with the analytical solution and the critical exponents determined by the numerical simulation obey the scaling laws (equation (10*a*)). These are good indicators that numerical solutions are reliable for recovering information about the thermodynamics of a system.

In the numerical solutions, if very small systems are considered, then no reliable information can be inferred (see for example the $L = 5$ curve in figure 2). And although the thermodynamic limit is impossible to achieve in numerical simulations, finite-size scaling techniques provide a useful tool to recover information about the critical exponents. This technique requires one to consider large systems in order to obtain solid information, but as we have stated before, in the scaling region, the critical slowing-down phenomenon is present, so sampling enough configurations requires a lot of MC steps. This problem is partially solved by using other algorithms that respect the detailed balance equations, but that improve the effectiveness of the algorithm update (instead of flipping one spin, clusters are flipped) so they reduce the critical slowing-down phenomenon [28–31].

So far we have seen that two particular situations emerge in the scaling region: the mean-field solution fails to reproduce the critical exponents and the numerical solution exhibits critical slowing-down. These situations illustrate the fact that in experiments is very hard to set the system at the critical point, it 'does not like to be' at the critical point, so critical phenomena (such as critical opalescence) are hard to achieve. This difficulty of being at the critical point is exhibited in the mean-field solution in the fact that performing an analytical expansion around the critical point fails; and in the numerical solution in the critical slowing-down, where it is difficult to sample enough configurations: the system does not 'feel comfortable' in the critical region. This 'unconformity' is understood in terms of the correlation length, because near the transition ξ diverges, so there is no length scale in the system and far regions in the system are correlated. This self-similarity its known as *coarsening*, which means is that if we take a picture of the system it will look statistically similar to a picture of the same system with another zoom. This correlation between far regions is what makes it difficult for numerical simulations to sample enough configurations and mean-field models to describe the singularity of the critical point.

Despite the fact that the phase transition can be 'visualized' in the order parameter, the correlation length ξ is the most important parameter in a phase transition because it defines the scale of the system. As pointed out earlier, the scaling laws, based on the scaling hypothesis [15] and proved by renormalization theory [16], are based on the fact that the singularity of a phase transition is carried by the correlation length, and that in the critical region the only length in the system that matters is ξ. Also, the finite-size scaling techniques are based on this fact. We can conclude that large spin clusters, but not the details over smaller scales, account for the physics of critical phenomena. An example of the importance of the correlation function and the correlation length is the Berezinskii–Kosterlitz–Thouless (BKT) phase transition which we will briefly discuss in section 8.

It is indispensable to mention that given a Hamiltonian it is relatively simple to adapt the numerical algorithm in order to sample states according to the appropriate probability distribution, and that the techniques presented for recovering thermodynamic quantities are the same regardless of the dimension of the system and its Hamiltonian. For example, the 3D

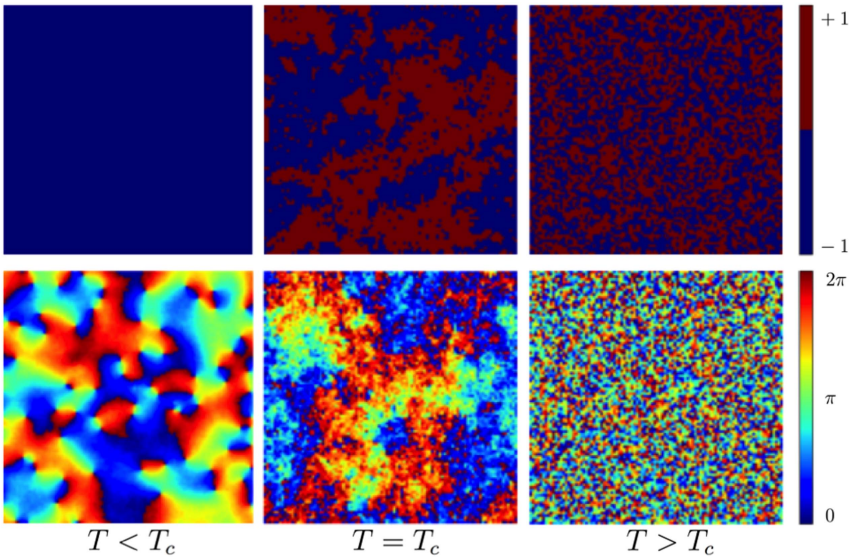

Figure 15. Behaviour of the 2D Ising model (top) and XY model (bottom) at $T < T_c$, $T = T_c$ and $T > T_c$. For the Ising model, an ↑ spin ($s_i = 1$) is represented by red and a ↓ spin ($s_i = -1$) is represented by blue. For the XY model, because every spin is determined by θ, so $\mathbf{s}_i = (\cos\theta, \sin\theta)$, an angle of 2π is represented by red and an angle of 0 by blue. In the low-temperature phase, the Ising model exhibits spontaneous magnetization while in the XY model vortex buddies appear (characterized by points where a continuum from blue to red, or vice versa, circle the point; it is worth noticing that these points are present by pairs with opposite circulation).

Ising model can be solved by using the same methods presented here, where the only difference is that the number of nearest neighbours is $z = 6$.

8. Beyond the Ising model: the XY model

In 1966 Mermin and Wagner proved that in certain 2D systems, such as the XY model, where in the Heisenberg Hamiltonian (1) the spin values are restricted to 2D unit vectors $\mathbf{s}_i = (\cos\theta, \sin\theta)$, there cannot be long-range order at a finite temperature [32].

What this means is that for all $T > 0$ the spin–spin correlation function does not become constant for large separation between spins, and the net magnetization vanishes.

However, in 1973, Kosterlitz and Thouless showed that despite there being no long-range order, there is a phase transition at finite temperature in such models [33]. The phase transition is not seen either in the system magnetization or in the specific heat or the magnetic susceptibility, but in the correlation function. For $T > T_c$ the spin–spin correlation function decreases exponentially, while for $T < T_c$ it falls off as a power law, as happens in a continuous phase transition at the critical temperature.

The XY model exemplifies the BKT transition. It is not a continuous phase transition like the one exhibited by the Ising model, because the order parameter (the magnetization) is zero

for any temperature and the specific heat and the magnetic susceptibility are not discontinuous at the transition, so it is referred to as an essential phase transition.

It is indeed true that there is no long-range order in the XY model, so Kosterlitz and Thouless proposed calling this order 'topological long-range order'. The BKT transition is characterized by the existence of vortices, which are bound in pairs of zero total vorticity (vortex buddies) below the critical temperature, while above it they are free to move under the influence of a weak applied magnetic field [33].

Vortices are the topological stable configurations in the XY model. Above the critical temperature unpaired vortices and anti-vortices may be present, and below it formation of vortex buddies occurs (a vortex and an anti-vortex are coupled). Thus, instead of spontaneous magnetization of the system, as happens in the Ising model, the presence of vortex buddies characterizes the BKT transition (see figure 15).

The 2D XY model is interesting because it is used to describe systems in condensed matter physics, such as superfluid helium films [33], superconducting films [34] and Josephson junction arrays [35], to cite a few examples amongst others. There is a lot of interest in explaining the phenomena previously presented, and in order to do so, the BKT transition must be understood, so many efforts are focused in this problem (see for example [36–39]).

9. Suggested problems

9.1. Implementing other algorithms

As a first problem, different types of algorithms may be implemented.

- **The Wolff algorithm.** This is a cluster algorithm, meaning that in every step spin clusters are flipped instead of in only one as in the Metropolis–Hastings algorithm. A nice discussion on how to do this for the Ising model is presented in [3, 31]. Reader should compare their results with those shown in figures 5 and 6 in order to understand how different the algorithms are. Readers should be able to reproduce figures 2–4 and 11. Interested readers could implement the Metropolis–Hastings and the Wolff algorithm for the XY model. In the Metropolis–Hastings algorithm each step is very similar as the one used for the Ising model, except that in each step an angle θ is proposed (instead of the flipping proposal) and ΔE_k calculated. For implementing the Wolff algorithm, see reference [30].
- **Continuous-time algorithm.** This is a variation of the Metropolis–Hastings algorithm in which in every step a spin in the lattice is chosen randomly, while in the continuous-time algorithm the spin in the lattice is chosen with a probability weighted in a proportional way to its probability of flipping. Thus once a spin is selected, the flipping is performed immediately (instead of having to compute the energy difference ΔE_k by scanning its neighbours) [40]. This algorithm can be easily implemented for $T = 0$ [41].

9.2. Higher-order spin Ising models

The Ising model is not restricted to square lattices and spin-$1/2$ systems, but has been extended to other geometries like triangular lattices [42, 43]. Physicists have not only played with the geometry, but with the nature of the interactions and the spin angular momentum as well.

The Blume–Emery–Griffiths (BEG) model is a spin-1 Ising model with a Hamiltonian given by [44],

$$\mathcal{H} = -J\sum_{\langle ij\rangle} \mathbf{s}_i \cdot \mathbf{s}_j - K\sum_{\langle ij\rangle} \mathbf{s}_i^2\mathbf{s}_j^2 - \Delta\sum_i \mathbf{s}_i^2, \tag{57}$$

that presents a rich variety of critical and multicritical phenomena [45] and has been extended to spin-3/2 systems [46–49]. The BEG model was introduced to simulate He^3–He^4 mixtures [44], but has been used to describe critical phenomena magnetic systems and multi-component fluids [50, 51].

We suggest that readers implement the Metropolis–Hastings algorithm for the Heisenberg Hamiltonian (1) for a spin-1 or spin-3/2 system and calculate E, M, C_H, χ_M and the correlation function, then compare their results with the spin-1/2 system. Later, implement the BEG model and observe what the 'multi-critical phenomena' means and how thermodynamic properties behave in this model.

10. Exotic applications of the Ising model

The Ising model has been used not only to model magnetic systems, but also binary alloy phase separations and simple lattice gauge theories amongst others. As an interesting case, social applications of the 2D Ising model have been found [52]. Its versatility and simplicity make the Ising model the first option for approaching new problems.

The results presented in the present paper are all equilibrium results mainly for undergraduate students. Nevertheless, graduate or advanced undergraduate students interested in this topic may find valuable non-equilibrium phase transitions [53], hysteretic responses in Ising ferromagnets [54], dynamical symmetry breaking [55] and also tricritical phenomena and stochastic resonance [56].

Acknowledgments

We would like to thank R Paredes, V Romero-Rochín and J A Seman for encouraging us to work on the problem, reading the manuscript and providing insightful comments, without their guidance and help this paper would probably not have existed. EI-G-P would like to thank V Romero-Rochín and CONACyT for the support as 'Ayudante de Investigador Nacional Nivel III' and FJP-C thanks SECITI-CLAF (SECITI 064/2015) for a postdoctoral fellowship.

References

[1] Brush S G 1967 *Rev. Mod. Phys.* **39** 883–93
[2] Tobochnik J 2001 *Am. J. Phys* **69** 255–63
[3] Sethna J P 2006 *Statistical Mechanics: Entropy, Order Parameters, and Complexity* (New York: Oxford University Press)
[4] Creutz M, Jacobs L and Rebbi V 1979 *Phys. Rev. Lett.* **42** 1390–3
[5] Ising E 1925 *Z. Phys.* **31** 253–8
[6] Onsager L 1944 *Phys. Rev.* **65** 117–49
[7] Istrail S 2000 Statistical mechanics, three-dimensionality and np-completeness: I. Universality of intractability for the partition function of the ising model across non-planar lattices *Proceedings of the 31st ACM Annual Symposium on the Theory of Computing, 21–23 May 2000,* (New York: ACM Press)
[8] Thijssen J 2007 *Computational Physics* 2nd edn (New York: Cambridge University Press)

[9] Krauth W 2006 *Statistical Mechanics: Algorithms and Computations* (New York: Oxford University Press)
[10] Binder K and Heermann D 2010 *Monte Carlo Simulation in Statistical Physics: An Introduction* 5th edn (Berlin: Springer)
[11] Mattis D C 1985 *The Theory of Magnetism II: Thermodynamics and Statistical Mechanics* (Berlin: Springer)
[12] Heisenberg W 1928 *Z. Phys.* **49** 619–36
[13] Mattis D C 1988 *The Theory of Magnetism I: Statics and Dynamics* (Berlin: Springer)
[14] Huang K 1963 *Statistical Mechanics* (New York: Wiley)
[15] Ma S K 2000 *Modern Theory of Critical Phenomena* (Boulder, CO: Westview)
[16] Wilson K G 1983 *Rev. Mod. Phys.* **55** 583–600
[17] Stoof H, Dickerscheid D and Gubbels K 2014 *Ultracold Quantum Fields Theoretical and Mathematical Physics* (Netherlands: Springer)
[18] ter Haar D 1965 *Collected Papers of L. D. Landau* (Oxford: Pergamon)
[19] Baxter R J 1982 *Exactly Solved Models in Statistical Mechanics* (New York: Academic)
[20] Strečka J and Jaščur M 2015 *Acta Phys. Slovaca* **65** 235–367
[21] Metropolis N, Rosenbluth A W, Rosenbluth M N, Teller A H and Teller E 1953 *J. Chem. Phys.* **21** 1087–92
[22] Hastings W K 1970 *Biometrika* **57** 97–109
[23] Glauber R J 1963 *J. Math. Phys.* **4** 294–307
[24] Landau D P 1976 *Phys. Rev.* B **13** 2997–3011
[25] Binder K 1981 *Z. Phys. B—Condens. Matter* **43** 119–40
[26] Binder K and Landau D P 1984 *Phys. Rev.* B **30** 1477–85
[27] Annett J F 2004 *Superconductivity, Superfluids and Condensates* (New York: Oxford University Press)
[28] Swendsen R H and Wang J S 1987 *Phys. Rev. Lett.* **58** 86–8
[29] Wolff U 1989 *Phys. Rev. Lett.* **62** 361–4
[30] Wolff U 1988 *DESY Report* 88–176
[31] Barkema G T and Newman M E J 1997 New Monte Carlo algorithms for classical spin systems *Monte Carlo Methods in Chemical Physics* (New York: Wiley) pp 483–517 (arXiv:cond-mat/9703179v1)
[32] Mermin N D and Wagner H 1966 *Phys. Rev. Lett.* **17** 1133–6
[33] Kosterlitz J M and Thouless D J 1973 *J. Phys.* C **6** 1181–203
[34] Beasley M R, Mooij J E and Orlando T P 1979 *Phys. Rev. Lett.* **42** 1165–8
[35] Rojas C and José J V 1996 *Phys. Rev.* B **54** 12361–85
[36] Hasenbusch M 2005 *J. Phys. A: Math. Gen* **38** 5869–83
[37] Bietenholz W, Gerber U and Rejón-Barrera F G 2013 *J. Stat. Mech: Theory Exp.* **2013** P12009
[38] Gerber U, Bietenholz W and Rejón-Barrera F G 2015 *J. Phys.: Conf. Ser.* **651** 012010
[39] Hsieh Y D, Kao Y J and Sandvik A W 2013 *J. Stat. Mech: Theory Exp.* **2013** P09001
[40] Bortz A, Kalos M and Lebowitz J 1975 *J. Comput. Phys.* **17** 10–8
[41] Lipowski A 1999 *Physica A* **268** 6–13
[42] Baxter R J and Wu F Y 1974 *Aust. J. Phys.* **27** 357–67
[43] Ranjbar S 2003 *Chin. J. Phys.* **41** 383–98
[44] Blume M, Emery V J and Griffiths R B 1971 *Phys. Rev.* A **4** 1071–7
[45] Horiguchi T 1986 *Phys. Lett.* **113A** 425–8
[46] Barreto F S and De Alcantara Bonfim O F 1991 *Physica* A **172** 378–90
[47] Kaneyoshi T and Jaščur M 1993 *Phys. Lett.* A **177** 172–6
[48] Bakchich A, Bassir A and Benyoussef A 1993 *Physica* A **195** 188–96
[49] Norihiro Tsushima Y H and Horiguchi T 1997 *J. Phys. Soc. Jpn.* **66** 3053–62
[50] Mukamel D and Blume M 1974 *Phys. Rev.* A **10** 610–7
[51] Lajzerowicz J and Sivardière J 1975 *Phys. Rev.* A **11** 2079–89
[52] Stauffer D 2008 *Am. J. Phys.* **76** 470–3
[53] Acharyya M 1998 *Phys. Rev.* E **58** 179–86
[54] Chakrabarti B K and Acharyya M 1999 *Rev. Mod. Phys.* **71** 847–59
[55] Acharyya M 2014 *J. Magn. Magn. Mater.* **354** 349–54
[56] Acharyya M 1999 *Phys. Rev.* E **59** 218–21